



NRL/FR/7180--00-9931

Blind Deconvolution to Improve Classification of Transient Source Signals in Multipath

LISA A. PFLUG
GEORGE B. SMITH
MICHAEL K. BROADHEAD

*Acoustic Simulation, Measurements, and Tactics Branch
Acoustics Division*

April 13, 2000

REPORT DOCUMENTATION PAGE

*Form Approved
OMB No. 0704-0188*

Public reporting burden for this collection of information is estimated to average 1 hour per response, including the time for reviewing instructions, searching existing data sources, gathering and maintaining the data needed, and completing and reviewing the collection of information. Send comments regarding this burden estimate or any other aspect of this collection of information, including suggestions for reducing this burden, to Washington Headquarters Services, Directorate for Information Operations and Reports, 1215 Jefferson Davis Highway, Suite 1204, Arlington, VA 22202-4302, and to the Office of Management and Budget, Paperwork Reduction Project (0704-0188), Washington, DC 20503.

1. AGENCY USE ONLY (<i>Leave Blank</i>)	2. REPORT DATE April 13, 2000	3. REPORT TYPE AND DATES COVERED Final	
4. TITLE AND SUBTITLE Blind Deconvolution to Improve Classification of Transient Source Signals in Multipath			5. FUNDING NUMBERS Program Element No. 62314N
6. AUTHOR(S) Lisa A. Pflug, George B. Smith, and Michael K. Broadhead			
7. PERFORMING ORGANIZATION NAME(S) AND ADDRESS(ES) Naval Research Laboratory Stennis Space Center, MS 39529-5004			8. PERFORMING ORGANIZATION REPORT NUMBER NRL/FR/7180--00-9931
9. SPONSORING/MONITORING AGENCY NAME(S) AND ADDRESS(ES)			10. SPONSORING/MONITORING AGENCY REPORT NUMBER
11. SUPPLEMENTARY NOTES			
12a. DISTRIBUTION/AVAILABILITY STATEMENT Approved for public release; distribution is unlimited.			12b. DISTRIBUTION CODE
13. ABSTRACT (<i>Maximum 200 words</i>) <p>General testing of several blind deconvolution techniques has indicated that one algorithm stands out as being the best choice for transient classification in shallow water. This is Cabrelli's algorithm, which was developed for oil and gas exploration in the seismic community. This work describes the algorithm and explores its applicability. Three aspects of performance were tested using simulation studies. The algorithm's ability to handle complicated transient signals was explored. Its ability to handle complex shallow-water environments was tested. Finally, its ability to perform adequately in noise was investigated. Studies using correlation coefficient comparisons of Cabrelli output to ground truth showed that the algorithm can handle complex environments, although it might not perform as well with complicated transient signals. Classification operating characteristics (CLOC) analysis showed that Cabrelli's algorithm performs adequately in noise.</p>			
14. SUBJECT TERMS Multipath Deconvolution Classification Blind			15. NUMBER OF PAGES 21
			16. PRICE CODE
17. SECURITY CLASSIFICATION OF REPORT UNCLASSIFIED	18. SECURITY CLASSIFICATION OF THIS PAGE UNCLASSIFIED	19. SECURITY CLASSIFICATION OF ABSTRACT UNCLASSIFIED	20. LIMITATION OF ABSTRACT UL

CONTENTS

1. INTRODUCTION	1
2. BLIND DECONVOLUTION TECHNIQUES	1
3. CABRELLI'S ALGORITHM	2
4. SIMULATIONS	5
4.1 Signal Complexity	6
4.2 Green's Function Complexity	7
4.3 Classification Performance Analysis	10
5. DISCUSSION	14
6. CONCLUSIONS	17
7. ACKNOWLEDGMENTS	17
REFERENCES	17

BLIND DECONVOLUTION TO IMPROVE CLASSIFICATION OF TRANSIENT SOURCE SIGNALS IN MULTIPATH

1. INTRODUCTION

Automated classification of transient source signals has become a necessity as Navy operations have shifted from the open ocean to the littoral environment. The multitude of transient signals received on a passive sonar system from biologics and surface vessels can overwhelm the sonar operator monitoring an area for targets of interest. Automation offers a means to identify and remove obvious false targets to significantly reduce the number of potential targets for the sonar operator to classify. A difficult problem even in simple cases, classification increases enormously in complexity when the received transient has been distorted by multipath, which can be significant at operational detection ranges in shallow water.

The received signal in the underwater multipath environment $x(t)$ is modeled by the convolution operation between the transient source signal $s(t)$ and a Green's function $g(t)$ that represents the multipath encountered by the source signal as it travels to the receiver. When $x(t) = s(t) * g(t)$ and $g(t)$ is known, deconvolution is used to obtain $s(t)$. Removing the multipath distortions in the signal, which are especially detrimental when multiple returns in the received signal overlap, allows more accurate classification of the source signal. Given the inherent uncertainties in underwater environmental data, it is virtually impossible to model a Green's function to represent multipath with sufficient accuracy for deconvolution to produce the correct source signal [1]. However, the source signal may be estimated using blind deconvolution. Blind deconvolution techniques do not require known Green's functions but instead use assumptions about the statistical properties of the Green's functions to obtain the source signal. One such technique is the subject of this report.

Section 2 of this report contains a more detailed description of the blind deconvolution problem in seismology and underwater acoustics and Section 3 gives one specific technique (the Cabrelli algorithm). Section 4 shows the results of some parameter studies using the Cabrelli algorithm and discusses the results of the simulation studies and future directions for research. Section 5 gives the conclusion.

2. BLIND DECONVOLUTION TECHNIQUES

Blind deconvolution is commonly used to mitigate multipath distortion that occurs over communication channels. It is also used to reduce blurring in image restoration. More closely related to the blind deconvolution problem in underwater acoustics is the seismic application, which attempts to retrieve the reflection coefficients for layers within the Earth without exact knowledge of the input waveform. The similarity is that in both the underwater acoustics and seismic applications, the multipath function (Green's function for underwater acoustics, reflectivity series for seismology) is well represented by a series of spikes interspersed with small, near-zero values. Each application assumes that the multipath function is "sparse."

One thoroughly investigated blind deconvolution technique proposed by the seismic community is the Wiggins' minimum entropy deconvolution technique [2]. This was the initial impetus for investigating the multipath problem in transient classification [3-5]. The Wiggins' method is now considered one of a series of cumulant maximization techniques [6, 7]. These techniques assume that the convolution of a multipath function with a source signal produces a received signal that is less sparse than the multipath function since

convolution is a smoothing process. The methods attempt to derive filters that drive the received signal to higher sparseness to obtain multipath functions that may then be used to implement deconvolution to obtain the source signal. Wiggins' measure of sparseness is the V -norm,

$$V(\mathbf{y}) = \sum_j y_j^4 / \left(\sum_j y_j^2 \right)^2,$$

which is essentially the same as kurtosis. Wiggins' technique can be recast using non-Gaussianity as the statistical feature of the multipath function that is reduced (i.e., made more Gaussian) by the process of convolution. Maximization of the V -norm leads to an iterative technique that has been shown to be quite sensitive to noise [8].

Later, Cabrelli [9] introduced a technique analogous to that of Wiggins in many respects. Most notably, Cabrelli's method uses the D -norm,

$$D(\mathbf{y}) = \max_{1 \leq j \leq m} |y_j| / \left(\sum_j y_j^2 \right)^{1/2},$$

as a measure of sparseness and, like the V -norm of the Wiggins' algorithm, the D -norm tracks closely with kurtosis. However, comparative studies show that the Cabrelli algorithm is less sensitive to noise than the Wiggins algorithm [5] and is better suited to the underwater acoustics application of blind deconvolution. Thus, the following presentation is limited to the Cabrelli method.

3. CABRELLI'S ALGORITHM

Cabrelli starts with a simple but reasonable signal model. The time series arriving at the j th hydrophone of an array is

$$x_j = s * g_j + n_j, \quad (1)$$

where s is the signal leaving the target of interest, g_j is the Green's function describing the propagation from the target to the j th hydrophone, and n_j is the noise on the j th hydrophone.

A filter f of length l is defined that acts on all of the data channels to produce filtered output,

$$y_j = f * x_j = f * s * g_j + f * n_j. \quad (2)$$

It is clear from Eq. (2) that a desirable filter would render the first term equal to the Green's function while correlating poorly with the noise term. Such a filter would be

$$f = s^{-1}, \quad (3)$$

since the first term would be rendered equal to the Green's function while s , and hence its inverse, is totally independent of the noise. If such a filter could be found, then the desired signal could be extracted as its inverse, and the Green's function estimate for each data channel could be found simply as the filtered data

$$y_j = f * x_j \cong s^{-1} * s * g_j = g_j. \quad (4)$$

Cabrelli attempts to find such a filter by assuming that the Green's functions are considerably sparser than the original data. The main assumption is that increasing the non-Gaussianity of the data will drive it toward the Green's function. Thus, by driving the sparseness of the original data up (by way of the filter f), Eq. (4), and hence, Eq. (3) could be satisfied. As a measure of sparseness, he used the simplicity or D -norm defined by

$$D(Y) = \max_{j,k} \left\{ \frac{|y_{j,k}|}{\|Y\|} \right\}, \quad (5)$$

where

$$\|Y\| = \sqrt{\sum_{j,k} y_{j,k}^2} \quad (6)$$

is the Euclidean norm of the matrix $Y = [y_{j,k}]$, and $y_{j,k}$ is the k th bin of the filtered data from the j th hydrophone. Cabrelli obtained this norm via geometric arguments, and showed the relationship of this norm with the varimax (kurtosis) norm used by Wiggins. Cabrelli argues that optimization of the D -norm will produce an estimate of a filter that satisfies Eqs. (3) and (4).

To optimize the D -norm, derivatives of $y_{j,k}$ and $\|Y\|$ will be required. These derivatives are easily calculated:

$$\frac{\partial y_{j,k}}{\partial f_m} = \frac{\partial}{\partial f_m} \left(\sum_n f_n x_{j,k-n} \right) = \sum_n x_{j,k-n} \frac{\partial f_n}{\partial f_m} = \sum_n x_{j,k-n} \delta_{nm} = x_{j,k-m}, \quad (7)$$

and

$$\begin{aligned} \frac{\partial \|Y\|}{\partial f_m} &= \frac{\partial}{\partial f_m} \sqrt{\sum_{j,k} y_{j,k}^2} = \frac{1}{2\|Y\|} \sum_{j,k} 2y_{j,k} \frac{\partial y_{j,k}}{\partial f_m} \\ &= \frac{1}{\|Y\|} \sum_{j,k} y_{j,k} x_{j,k-m} = \|Y\|^{-1} \sum_{j,k,n} f_n x_{j,k-n} x_{j,k-m}. \end{aligned} \quad (8)$$

It will be convenient later to express this latter derivative in terms of the data autocorrelations,

$$\Gamma_{n-m} = \sum_{j,k} x_{j,k-n} x_{j,k-m}, \quad (9)$$

as

$$\frac{\partial \|Y\|}{\partial f_m} = \|Y\|^{-1} \sum_n f_n \Gamma_{n-m}. \quad (10)$$

To optimize the D -norm, the normal equations for the filter coefficients are obtained by setting the derivatives with respect to the filter coefficients equal to zero. This gives

$$\frac{\partial}{\partial f_m} \left[\frac{y_{j,k}}{\|Y\|} \right] = \|Y\|^{-2} \left[\|Y\| \frac{\partial y_{j,k}}{\partial f_m} - y_{j,k} \frac{\partial \|Y\|}{\partial f_m} \right] = 0, \quad (11)$$

which can be written as

$$x_{j,k-m} - y_{j,k} \|Y\|^{-2} \sum_n f_n \Gamma_{n-m} = 0, \quad (12)$$

where Eqs. (7) and (10) have been used and where j runs over hydrophones while k runs over bins.

By constructing an autocorrelation matrix R whose elements are given by

$$R_{nm} = \Gamma_{n-m}, \quad (13)$$

the normal equations can be written in matrix form as

$$y_{j,k} \|Y\|^{-2} R \cdot f = x^{jk}. \quad (14)$$

f is a column vector composed from the filter coefficients, and x^{jk} is the transpose of $[x_{j,k}, x_{j,k-1}, \dots, x_{j,k-1}]$, with $x_{j,n} = 0$ if n does not correspond to a bin number.

Notice that the normal equations are invariant under the scale transformation $f \rightarrow \lambda f$, where λ is a scalar multiple. Since $y_{j,k} \|Y\|^{-2}$ is a scalar, then the simpler equation

$$R \cdot f = x^{jk} \quad (15)$$

has the same solution set as the original normal equations.

Assuming that R is well conditioned for inversion,

$$f^{jk} = R^{-1} \cdot x^{jk} \quad (16)$$

is evaluated for the set of filters (one for each j,k pair), each filter is applied to the original data to get

$$y_{m,i}^{jk} = \sum_n f_n^{jk} x_{m,i-n}, \quad (17)$$

and the matrix $Y^{jk} = [y_{m,i}^{jk}]$ is formed for each jk pair.

Equation (5), in the form

$$D = \max_{jk} \left\{ \left| \frac{y^{jk}}{\|Y^{jk}\|} \right| \right\}, \quad (18)$$

can now be evaluated to select the optimum filter from the set $\{f^{jk}\}$. The optimum filter is then inverted to give the signal estimate. If the Green's functions are desired, they are given by the y_m^{jk} used to compose Y^{jk} for the optimal jk pair that has already been calculated to evaluate the D -norm in Eq. (18).

Cabrelli denotes the process just described as

$$\sup_f \{D\} = \sup_f \left\{ \max_{j,k} \left\{ \frac{|y_{j,k}|}{\|Y\|} \right\} \right\} = \max_{j,k} \left\{ \sup_f \left\{ \frac{|y_{j,k}|}{\|Y\|} \right\} \right\}. \quad (19)$$

The first statement in Eq. (19) says to choose the filter that optimizes the D -norm—an obvious statement of the problem. However, the second statement says that the operations are interchangeable and that it is much simpler to find a set of optimal filters (one for each jk pair) and then pick the one that maximizes the D -norm. This process is described by Eqs. (16) through (18).

4. SIMULATIONS

This report gives three basic simulation analyses of the Cabrelli algorithm:

- (1) Cabrelli performance vs signal complexity,
- (2) Cabrelli performance vs Green's function complexity, and
- (3) a classification operating characteristics (CLOC) analysis of Cabrelli performance vs signal-to-noise ratio (SNR).

In all three studies the received data were simulated according to Eq. (1) by convolving artificially constructed transient signals with artificially constructed Green's functions. Noise was added only in the third study. The constructed transients and Green's functions were different for each of the three studies and are described separately for each study.

Performance of the Cabrelli algorithm was evaluated by calculating a normalized correlation between the transient signal that Cabrelli's algorithm estimates and the actual transient used to simulate the data. The normalization was performed according to

$$\gamma(a,b) = \frac{\max(a \otimes b)}{\sqrt{\max(a \otimes a)} \cdot \sqrt{\max(b \otimes b)}}, \quad (20)$$

(where \otimes represents correlation) for the normalized correlation between two signals a and b . Although most classifiers are generally much more sophisticated and involve many signal features, this performance measure is adequate for these studies that compare only the quality of the source estimate with no processing (the received signal) with the source estimate obtained from the blind deconvolution algorithm.

It is assumed that the passband of the received signal has been estimated prior to this stage of processing. With this assumption, the received signal was bandpass filtered before it was sent to the Cabrelli algorithm, and the signal estimate produced by the Cabrelli algorithm was again bandpass filtered before it was sent to the classifier (i.e., before the normalized correlation was calculated).

4.1 Signal Complexity

The waveform type that Cabrelli originally developed his algorithm for was the simple wavelet signal commonly used in seismic petroleum exploration. This naturally raises the concern that this algorithm might not perform adequately when it is used with the more complicated transient signals commonly encountered in underwater acoustics. To study the effect of signal complexity on Cabrelli performance, complexity must first be defined.

Cabrelli's algorithm does not perform well for hyperbolic frequency-modulated (HFMs) or linear frequency-modulated (LFMs) signals. Since it does work well on continuous wave (CW) signals, the question arises: How does its performance behave as a function of signal bandwidth? Thus, the bandwidth of an LFM with a fixed center frequency was used as the measure of complexity.

A series of 100-ms LFMs were produced, each one centered on 100 Hz with bandwidths increasing from 0.001 to 180 Hz. These trial LFMs were convolved with a set of synthetic Green's functions from the set described in the next section to make a set of received signals at the three hydrophones of an array. The Cabrelli algorithm was applied to each member of this set for all reasonable filter lengths, and the correlations of the outputs with their corresponding transients were calculated using Eq. (20). Figure 1 shows the maximum correlation (over filter length) plotted against bandwidth. The trend to poor performance at high bandwidth for LFM signals is clearly demonstrated by this figure. The same trend is observed in Fig. 2 for the correlations averaged over Green's functions.

Why does this degradation occur? One possibility is that the simplicity as measured by the D -norm might increase as bandwidth increases. If the D -norm of the simulated transient (without multipath) is com-

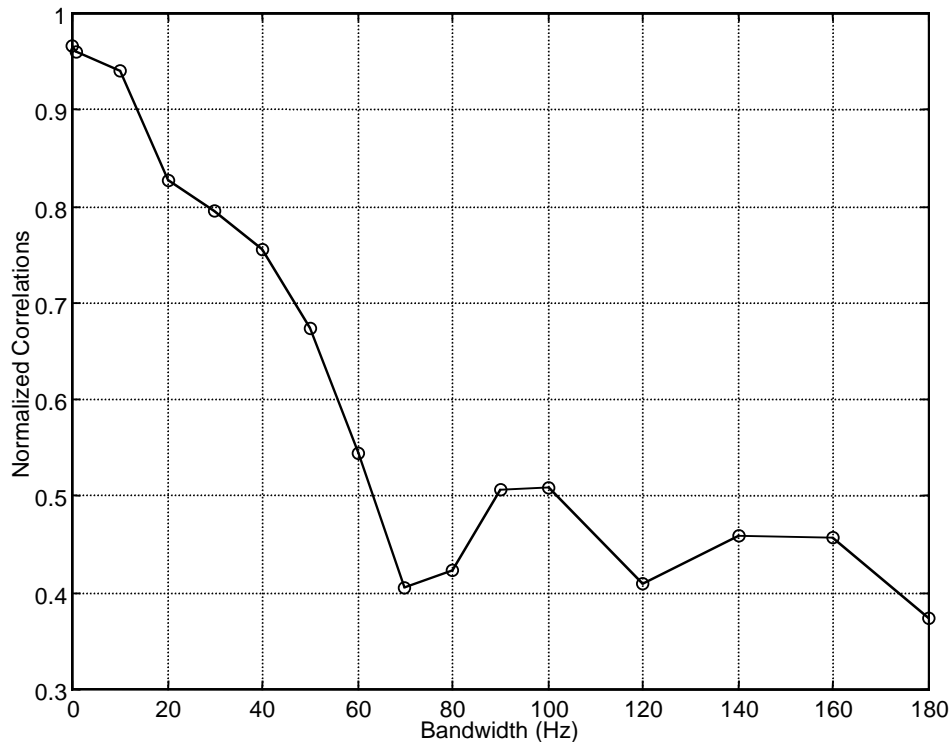


Fig. 1 — Normalized correlations of the transient signals extracted by Cabrelli's algorithm with the simulated transient signal used to construct the data as a function of signal complexity as measured by the bandwidth of the LFM used in this study

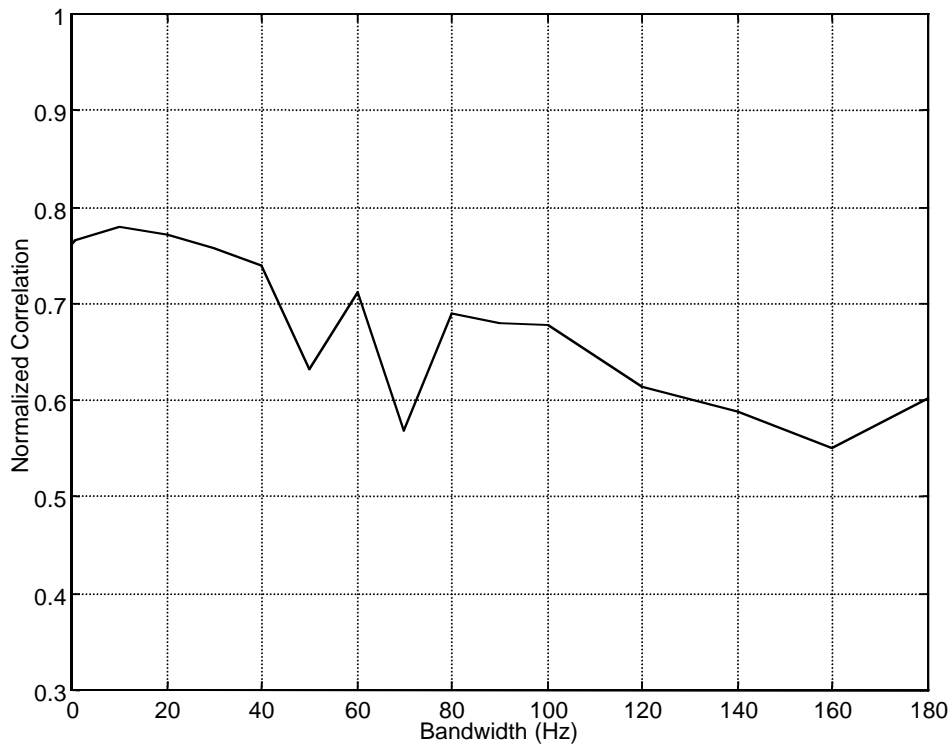


Fig. 2 — Normalized correlations of the Green’s functions extracted by Cabrelli’s algorithm for hydrophone 3 with the simulated Green’s functions used to construct the data as a function of the bandwidth of the LFM used in this study

parable to the D -norm of the Green’s function, the performance of Cabrelli’s algorithm might be compromised. Figure 3 shows the D -norm of the simulated transient prior to convolution with the Green’s function plotted against bandwidth. The simplicity increases with increasing bandwidth from about 0.135 to about 0.1455, but this change in the D -norm across the bandwidth explored is relatively small. This change was only about 0.0105, approximately 3% of the variation in D -norm usually encountered in the loop over jk pairs performed in the Cabrelli algorithm. The D -norms for the Green’s functions were 0.55, 0.25 and 0.28. At the low bandwidth end, the ratios of transient D -norms to Green’s functions D -norms for the three hydrophones were 24%, 54%, and 49%. At the high end, they were 26%, 58%, and 52%. It would be hard to imagine that this slight increase in the percentages would produce such a noticeable change in performance.

4.2 Green’s Function Complexity

The type of Green’s function for which Cabrelli originally developed his algorithm was the extremely sparse “reflection time series” commonly found in seismic petroleum exploration. These Green’s functions are zero almost everywhere, with only a few nonzero spikes which are usually well spaced. This fact naturally raises the concern that Cabrelli’s algorithm might not perform adequately (or even at all) when it is used with the vastly more complicated Green’s functions commonly encountered in shallow-water acoustics. Two Green’s function complexity studies were done. The first used artificial Green’s functions of increasing complexity, while the second used Green’s functions constructed with the SACLANTCEN Normal-Mode Acoustic Propagation Model (SNAP) using the environmental parameters from a range independent run from an acoustically shallow site in the Atlantic Ocean near the Blake Plateau [10]. This latter set of Green’s functions was made more complex in a realistic way by increasing the range from the target to the receiver; range was the complexity measure.

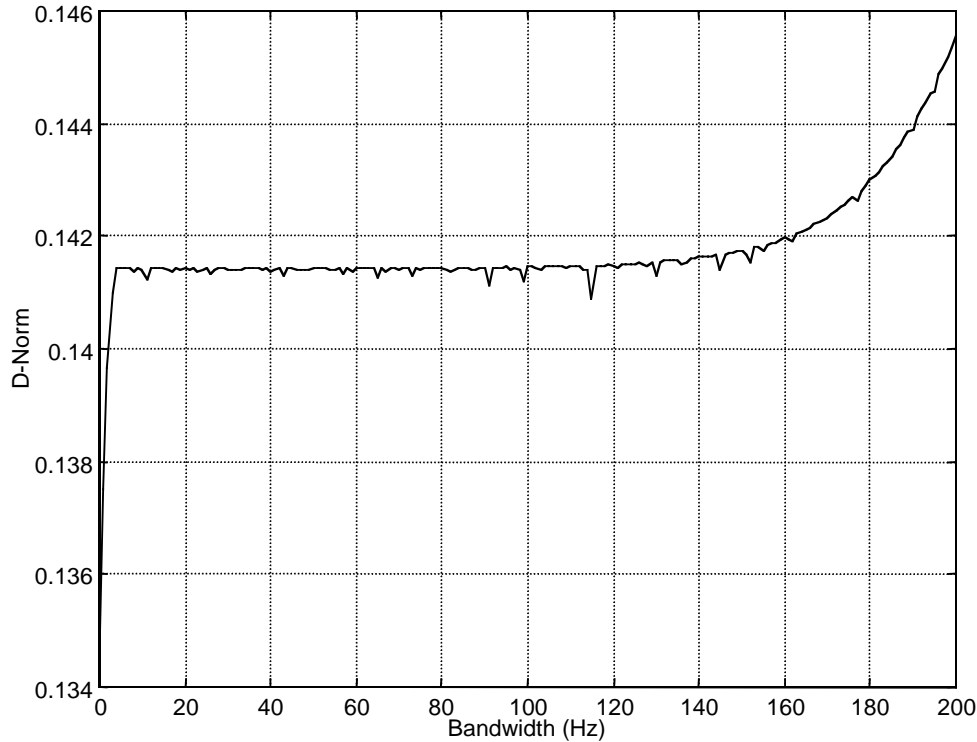
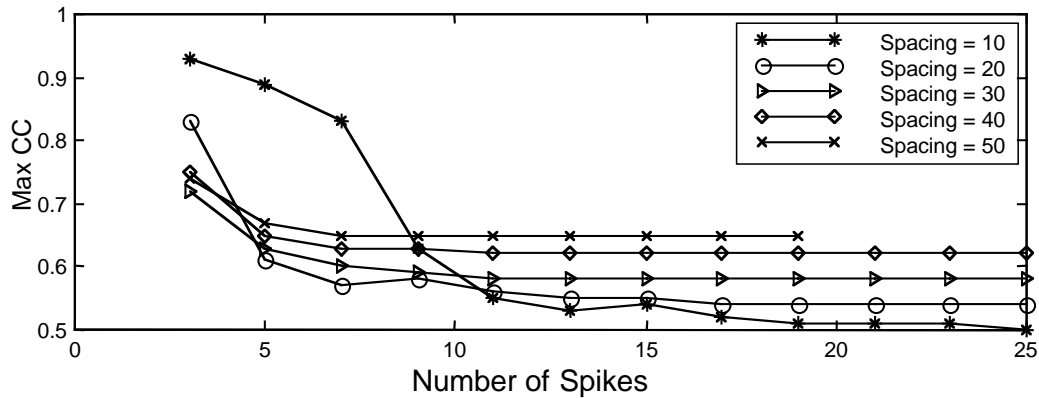


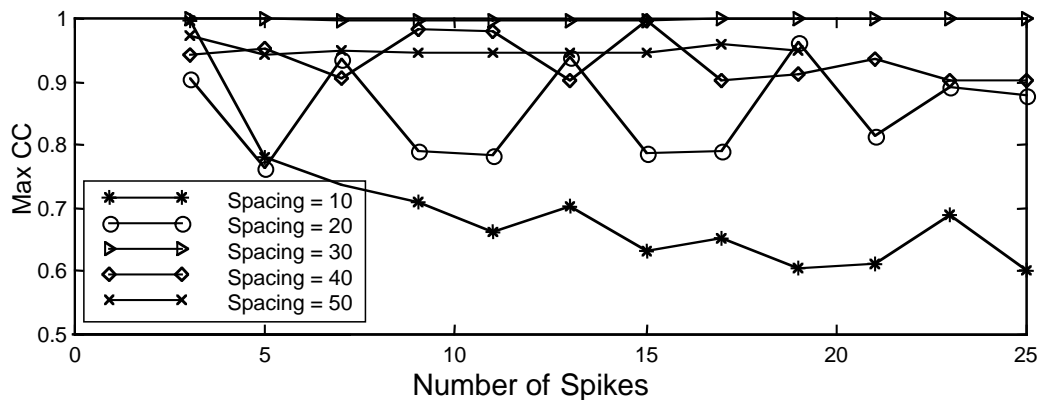
Fig. 3 — Values of the D -norm for the transient signals used to construct the data as a function of the bandwidth of the signals

The artificial Green's functions consisted of 3 to 25 alternate-sign spikes modified with an exponential decay to simulate decreasing size of returns with increasing range imposed on a sequence of 1000 zeros. The spacing between spikes was prescribed at 10, 20, 30, 40, and 50 bins. The signal used was a 300-pt metallic bang (i.e., an exponentially damped sinusoid centered on a frequency of 20 Hz). A single hydrophone was simulated.

Figure 4(a) shows a plot of the normalized correlations between the source estimate and the true source vs the number of spikes in the Green's function for the case of no deconvolution. The multiple traces on this plot correspond to different spike spacings. Figure 4(b) shows the same calculations for source estimates obtained from the blind deconvolution technique. Figure 4(a) shows what might be expected—performance degrades as the complexity of the Green's functions increases. Except for an initial result with the 10-point spacing and a 3-spike Green's function, the correlation coefficients are less than 0.9, and for simulated Green's functions with 9 or more spikes, the correlation coefficients are less than 0.7. Figure 4(b) shows performance oscillating as the complexity of the Green's functions increases. The oscillation is probably an artifact caused by the regular spacing of the spikes in the artificial Green's functions, but the lack of a degrading trend as the number of spikes is increased (except for the 10-bin spacing) is encouraging. The exceptional performance that occurs with a spacing of 30 bins is an artifact of the processing and should not be regarded as expected behavior. The original damped sinusoid has a 15-bin periodicity, and the 30-bin spacing between Green's function spikes results in constructive interaction in the convolution process. The Green's function spikes line up with the sinusoid peaks, leading to high correlations in this example. With a phase shift in the damped sinusoid, the Green's function spikes could line up small values within the sinusoid and result in correlations that are stable with increasing spike number but significantly lower than that shown.



(a) No preprocessing



(b) Cabrelli preprocessing

Fig. 4 — Maximum values (over filter length) of the normalized correlations as functions of Green's function complexity as measured by the number of spikes in the Green's functions

The second Green's function complexity study uses the same metallic bang but more realistic Green's functions to form the multipath corrupted received signals that would be used for classification. The Green's functions were obtained using the SNAP normal mode model at differing ranges to produce a set of received signals on an array of 16 hydrophones for each range. The unprocessed source signal estimates were processed using Cabrelli's algorithm, and the output was compared to the initial transient signal using Eq. (20) for a range of filter lengths. Figure 5 shows the result.

This figure plots correlations vs filter length and range. At each range, filter length can be scanned to see if there are any filter lengths that produce correlations greater than the unprocessed correlation (which is plotted vs range in the left-most column of the figure). As the ranges of Fig. 5 are examined, it becomes apparent that at the smallest ranges (600 and 2400 m) Cabrelli output is no better than the unprocessed signal. This is not surprising since at these ranges there is very little multipath corruption of the signal.

At 4300 m, the unprocessed signal correlates poorly with the initial transient, but there is a range of filter lengths around 40 m for which the Cabrelli estimated source signal is significantly better than the unprocessed signal. (The small filter lengths are ignored because the signal extracted from such a short filter would not have enough points to give an adequate representation of the initial transient.) As the rest of the ranges are scanned, it becomes clear that at any range there are always sufficiently large filter lengths for

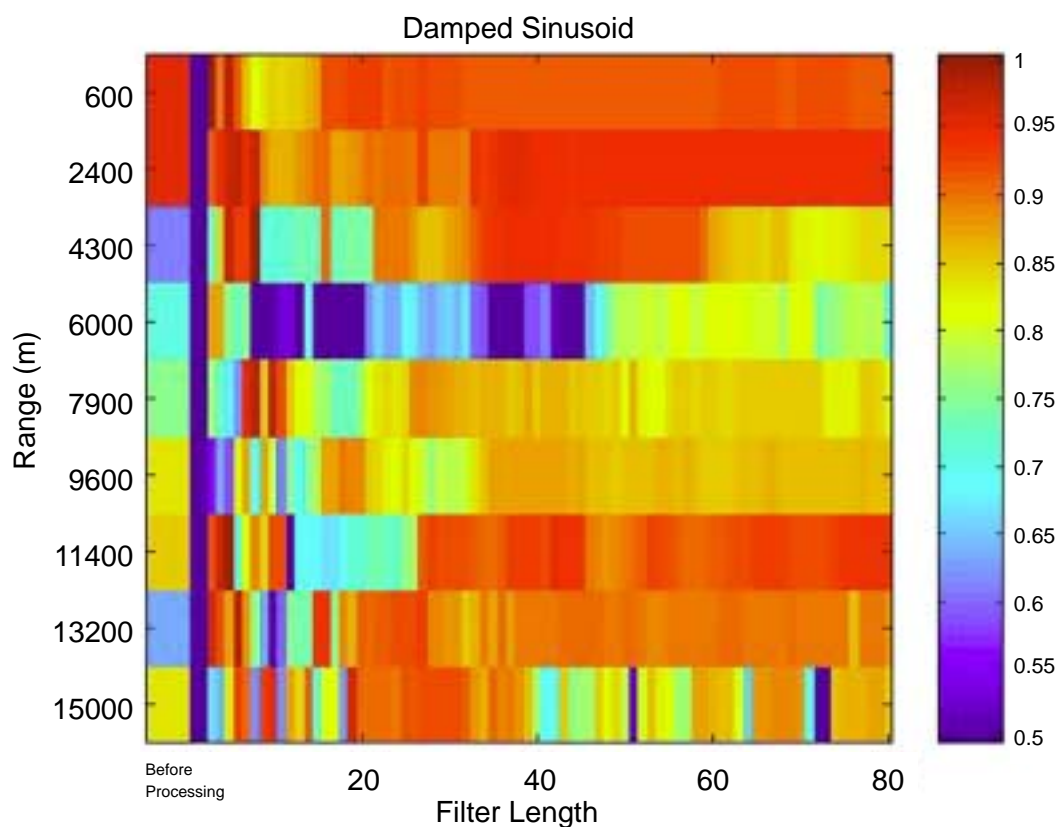


Fig. 5 — Normalized correlations of the signals extracted from Cabrelli preprocessing with the transient signals used to construct the data as functions of filter length and target range that were used as a measure of Green's function complexity

which application of the Cabrelli algorithm would be better than no preprocessing. The conclusion that Cabrelli's algorithm can perform adequately with Green's functions of the complexity found in shallow water at tactical ranges is justified.

4.3 Classification Performance Analysis

In this study, the Cabrelli algorithm was run using five different signals that represent five different classes of transients. Noise levels at five SNRs were tested, with SNR defined as the ratio of signal and noise standard deviations and converted to decibels (dB) for display. The signal types are labeled Bang, Pulse, LFM, Sumsin and PRN.

The bang is an exponentially damped sinusoid centered on 60 Hz. The pulse is constructed to have a flat (real) spectrum from 25 to 75 Hz. The LFM is a 333-ms sweep from 30 to 90 Hz. Sumsin is a sum of two sine waves at 30 and 33 Hz, with the second one phase-shifted to make the transient taper at its extremities. The PRN contains uniformly distributed, zero-mean white noise bandpass filtered to the band from 20 to 70 Hz. All of these signals were zero padded with as many zeros preceding them as there were bins in the nonzero part of the signal and with the same number of zeros following them.

A single set of SNAP-generated Green's functions from Section 4.2 (one for the propagation to each hydrophone) was used to create received signals at a range of 11400-m for use in this study. The 11400-m range was chosen because it presents significant multipath corruption and corresponds to good results for the performance of the Cabrelli algorithm. As an example of the degree of multipath corruption in each of

the five signals, Fig. 6 shows the five simulated transients next to one channel of received data for the 11400-m range.

Twenty realizations of the noise were mixed with each of the five received signals at a fixed SNR. These 100 prepared signals were each run through the Cabrelli algorithm for a set of reasonable filter lengths (the l in the definition of the x^{jk} used in Eqs. (14) and (15)), and the optimal filter length was chosen for each signal, based on correlations with the true source. In practice, the optimum filter length is unknown (see Section 5, Discussion), but it is assumed to be known in this study to illustrate the best possible performance for the algorithm.

The 100 resulting output signal estimates were compared with the five trial transients using the correlation (Eq. (20)). The 500 resulting correlations were used to populate a confusion matrix. A confusion matrix has the signal type for the unidentified source labeling the rows and classification choices labeling the columns.

Figure 7 shows the data used to construct a confusion matrix for this study, corresponding to an SNR of 15 dB. The plot in each block of this 5×5 matrix shows the correlations for that box plotted in increasing order. For each threshold value, the counts from each block can be easily ascertained visually. These counts are needed to calculate probabilities. The diagonal blocks represent correct classifications (or false

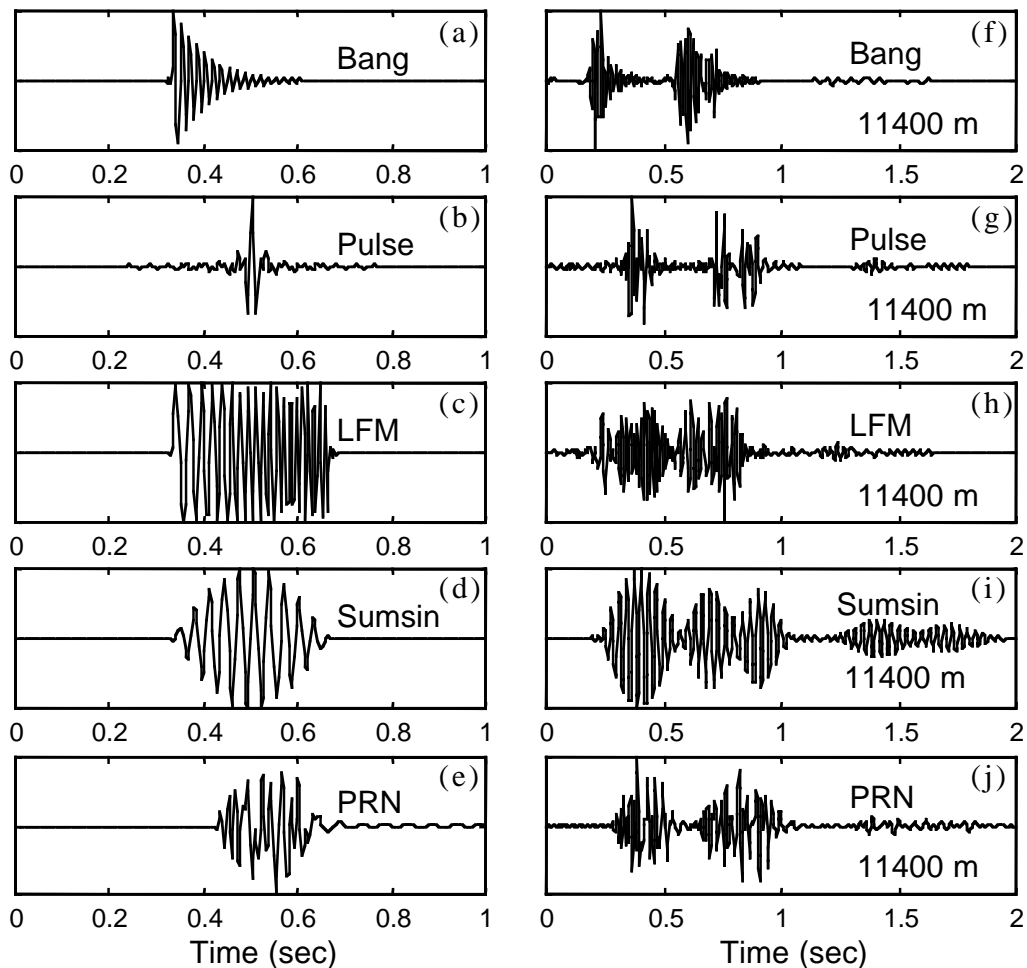


Fig. 6 — Five classes of transient signals (a) through (e), and the received transients at the 11400-m range (receiver depth of 96 m) (f) through (j)

dismissals), while off-diagonal blocks represent false classifications (or correct dismissals). A confusion matrix is judged “good” if correlation values in its diagonal blocks are large and the correlation values in its off-diagonal blocks are small.

Four probabilities can be calculated from Fig. 7 by counting the numbers of correlations above and below a threshold value and normalizing by the number of possible outcomes.

These four probabilities for a given prepared signal type are:

P_{cc} = (probability of correct classification)—number of correlations *above* threshold in diagonal block/number of realizations,

P_{fc} = (probability of false classification)—number of correlations *above* threshold in rest of row/(number of signal types-1)(number of realizations),

P_{cd} = (probability of correct dismissal)—number of correlations *below* threshold in rest of row/(number of signal types-1)(number of realizations), and

P_{fd} = (probability of false dismissal)—number of correlations *below* threshold in diagonal block/number of realizations.

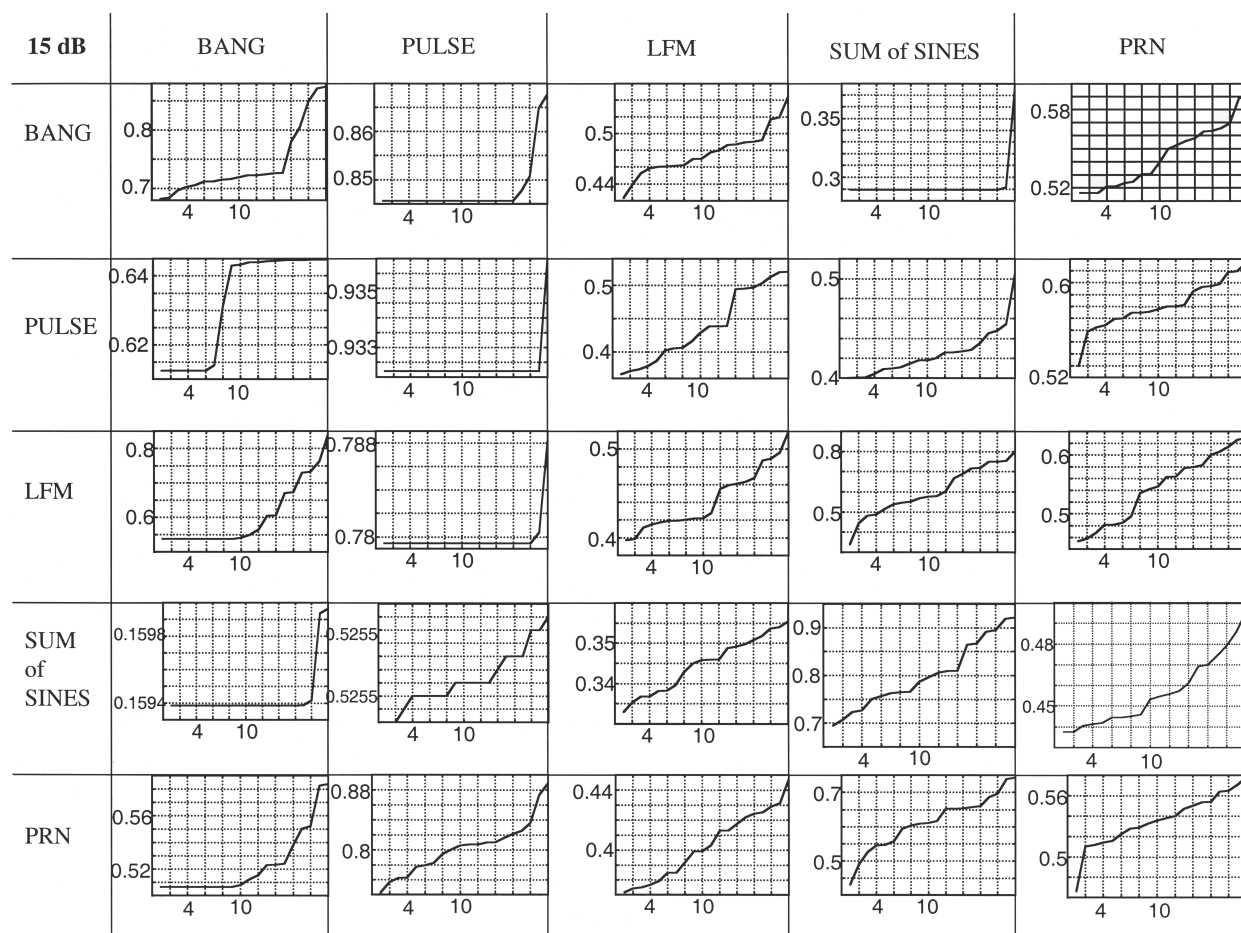


Fig. 7 — Confusion matrix for an SNR of 15 dB from the CLOC analysis. The graph in each square of the matrix shows the correlations over 20 realizations. Counts of correlations above and below a given threshold can be read visually from this figure for the construction of CLOC curves.

If a particular correlation value is greater than the threshold value, it is counted as a classification. If it is less than the threshold value, it is counted as a dismissal.

Each probability could be plotted against the threshold value or, as is more common, parametric plots of one probability vs another could be made. Note that the scales on the plots of correlation values in Fig. 7 are not consistent across subplots but are scaled to be relevant for each particular case. In many cases, the correlation values are below 0.8, which in general represents poor correlation for these signals.

Tables 1 through 10 give the confusion matrices resulting from use of the maximum correlation as the classification criterion for the five different SNRs. Each element contains the number of realizations (out of 20) for which the signal heading each column is chosen by the classifier. When all five signal classes are used for classification, as done in Tables 1 through 5, the pulse and Sumsin signals are properly classified with high probability (implies high P_{cc}) at all SNRs. In no instance is the signal improperly dismissed (implies low P_{fd}). However, the bang, LFM, and PRN are almost as likely to be falsely classified (implies high P_{fc}) as the pulse or Sumsin, as these two signals are to be correctly classified. Removing the pulse and Sumsin signals from the classification classes results in high P_{cc} and low P_{fd} for the bang, but the LFM is falsely classified as the bang well over 50% of the time; it is falsely classified as the PRN the remainder of the time. The PRN is somewhat better with higher correct classifications at the high SNRs.

Table 1 — Five-Class Confusion Matrix for SNR = 5 dB

	Bang	Pulse	LFM	Sumsin	PRN
Bang	0	19	0	1	0
Pulse	0	20	0	0	0
LFM	2	17	0	1	0
Sumsin	0	0	0	20	0
PRN	0	20	0	0	0

Table 2 — Five-Class Confusion Matrix for SNR = 10 dB

	Bang	Pulse	LFM	Sumsin	PRN
Bang	0	20	0	0	0
Pulse	0	20	0	0	0
LFM	2	17	0	1	0
Sumsin	0	0	0	20	0
PRN	0	19	0	1	0

Table 3 — Five-Class Confusion Matrix for SNR = 15 dB

	Bang	Pulse	LFM	Sumsin	PRN
Bang	3	17	0	0	0
Pulse	0	20	0	0	0
LFM	1	18	0	1	0
Sumsin	0	0	0	20	0
PRN	0	20	0	0	0

Table 4 — Five-Class Confusion Matrix for SNR = 20 dB

	Bang	Pulse	LFM	Sumsin	PRN
Bang	0	20	0	0	0
Pulse	0	20	0	0	0
LFM	0	20	0	0	0
Sumsin	0	0	0	20	0
PRN	0	20	0	0	0

Table 5 — Five-Class Confusion Matrix for SNR = 25 dB

	Bang	Pulse	LFM	Sumsin	PRN
Bang	1	19	0	0	0
Pulse	0	20	0	0	0
LFM	0	18	0	2	0
Sumsin	0	0	0	20	0
PRN	0	20	0	0	0

Finally, Classification Operating Characteristics (CLOC) curves for the five SNRs are shown for the five signals in Fig. 8. These curves include only two of the probabilities (i.e., P_{cc} and P_{fc}) and are created by varying a threshold correlation value and calculating the probabilities as defined above. The pulse and Sumsin signals in (b) and (d) are classified correctly with P_{cc} reaching 1.0, while P_{fc} is still zero. The bang in (a) reaches a P_{fc} of between 0.3 and 0.4 before P_{cc} reaches 1.0. However, the remaining two signals (c) and (e) reach P_{fc} values of about 0.7 to 1.0 and 0.35 to 0.45 before P_{cc} reaches 1.0.

5. DISCUSSION

The results of the previous sections show that Cabrelli's algorithm performs well with complicated propagation Green's functions of the type common to tactical ranges in a shallow-water environment over a range of reasonable SNRs. However, it is quite sensitive to signal type and signal complexity that increases with frequency. While this study shows that there are two signal types for which the algorithm improves correct classification with high probabilities (pulse and Sumsin), the degree to which this will improve a classifier for the pulse is limited by high probabilities for false classification of the remaining signals. The algorithm generates source signal estimates for the received bang, LFM, and PRN signals that are just as likely to be classified as a pulse as is the received pulse. The pulse appears to be the "default" estimate.

Using only the bang, LFM, and PRN signal classes, the bang was always correctly classified as a bang (see Tables 6 through 10). Unfortunately, the PRN was also classified as a bang in a significant number of the cases for the five SNRs (17, 13, 5, 12, and 9 times out of 20, respectively). However, the PRN was correctly classified in the remaining cases. Even with only three choices, the LFM was never classified as an LFM but as a bang and occasionally as a PRN.

The results given in this report are dependent on the correlation as the classifier. Therefore, they are not sufficient to draw complete conclusions about the improvements that the Cabrelli algorithm may have on classification. For example, when the bang is falsely classified as the pulse, the source estimate generated by the Cabrelli algorithm is visually something in between the two signal types, as illustrated in Fig. 9. Here, the source estimate derived from the received bang in the 11400-m case from the earlier section is

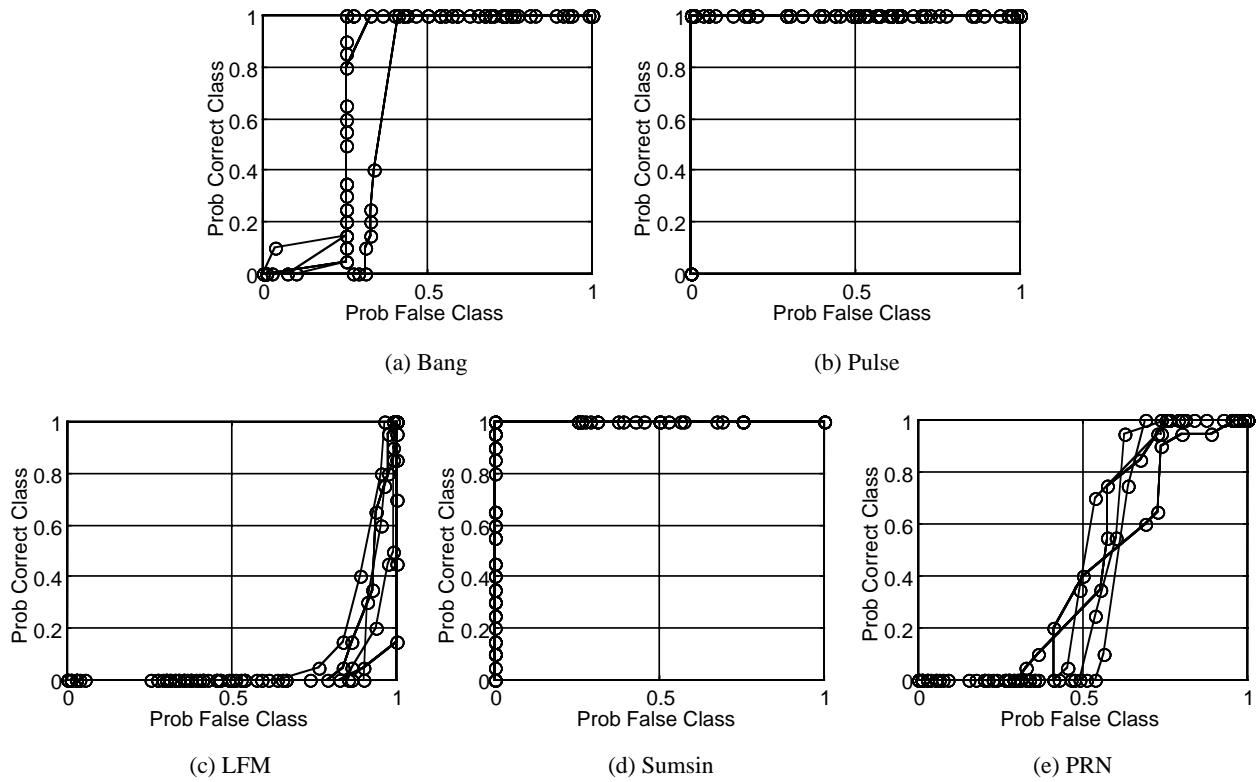


Fig. 8 — CLOC curves (the five curves in each subplot represent SNR values of 5, 10, 15, 20, and 25 dB)

Table 6 — Three-Class Confusion Matrix for SNR = 5 dB

	Bang	LFM	PRN
Bang	20	0	0
LFM	16	0	4
PRN	17	0	3

Table 7 — Three-Class Confusion Matrix for SNR = 10 dB

	Bang	LFM	PRN
Bang	20	0	0
LFM	16	0	4
PRN	13	0	7

Table 8 — Three-Class Confusion Matrix for SNR = 15 dB

	Bang	LFM	PRN
Bang	20	0	0
LFM	12	0	8
PRN	5	0	15

Table 9 — Three-Class Confusion Matrix for SNR = 20 dB

	Bang	LFM	PRN
Bang	20	0	0
LFM	12	0	8
PRN	12	0	8

Table 10 — Three-Class Confusion Matrix for SNR = 25 dB

	Bang	LFM	PRN
Bang	20	0	0
LFM	16	0	4
PRN	9	0	11

more correlated with the pulse signal rather than the bang, but other classification features might easily recognize it as the bang.

So far, the issue of filter length has been ignored. There are different approaches to dealing with this unknown parameter. The first approach is to directly pass the source estimates generated for each filter length to the classifier. An alternate approach is to cull the source estimate set to a significantly smaller set before passing to the classifier. For example, if the hydrophones are separated such that the Green's func-

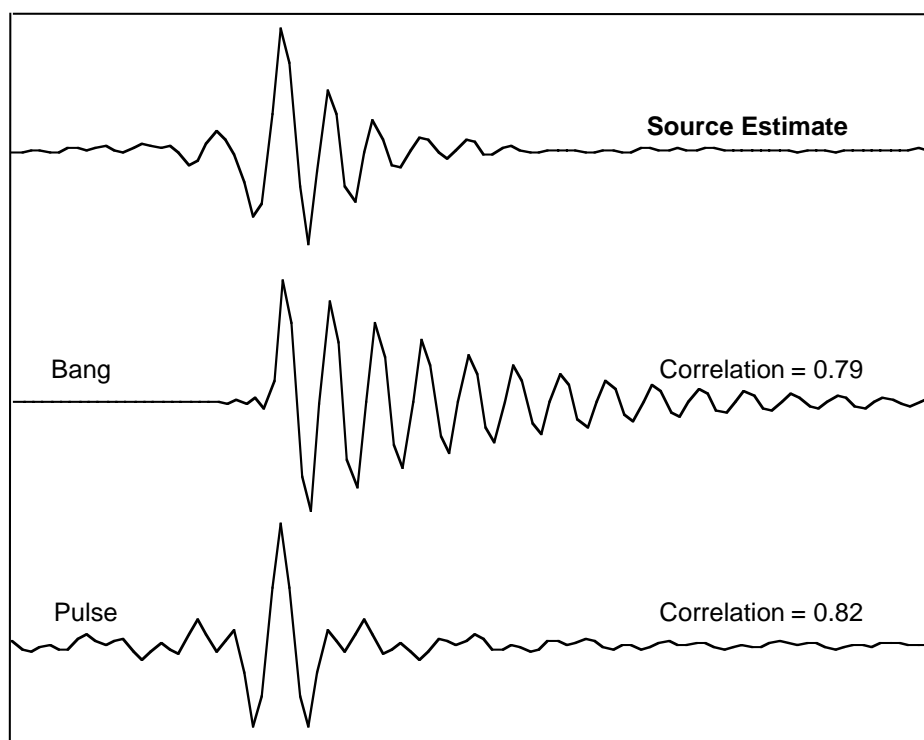


Fig. 9 — Source estimate generated by the deconvolution algorithm for the received bang signal compared to the bang and the pulse

tions are significantly different from channel to channel, then the average autocorrelation of the received signals will be similar to the autocorrelation of the source signal. This average autocorrelation can be used to reduce the size of the solution set by comparing the autocorrelations of the extracted signals with the autocorrelations of the classification signal types. Also, exploratory studies have shown that for some signal types, the best source estimate often appears at multiple filter lengths, while the other estimates are dissimilar. This redundancy can be exploited to cull the solution set. However, any sort of culling before classification introduces more uncertainty into the problem. As long as the classifier operates quickly, it is the most reliable way to cull the solution set. Thus, at the expense of higher P_{fc} , it is perhaps better to pass the entire source estimate set directly to the classifier.

Clearly, the Cabrelli algorithm alone will not be adequate as a general multipath compensation preprocessor in shallow-water transient classification. It will have to be aided in some way, and this research now takes this direction. Other algorithms under investigation use information that is independent of the information that Cabrelli's algorithm uses. For example, Rietsch's algorithm [11] uses the fact that the signal is common to all hydrophones of an array, while the Green's functions are different from element to element. This algorithm can handle any signal (no matter how complicated) and any Green's function, but it is too sensitive to noise in its present incarnation. Ways are being explored (with some success) to stabilize it against noise. An algorithm derived from a joint "cost" function that uses stochastic information from Cabrelli's algorithm and deterministic information from Rietsch's algorithm (or other deterministic algorithms) should produce significantly improved results and be stable in noise.

6. CONCLUSIONS

The Cabrelli algorithm for blind deconvolution has been elucidated and tested with simulated multipath corrupted transient data. It was found to be insensitive to the complexity of the Green's function describing the propagation, relatively robust against noise, but very sensitive to signal type and signal complexity. Specifically, it was found to be a good preprocessor for the classification of pulses and sums of sines, but it performed poorly with metallic bangs, LFM's, and PRN's. The probability of false classification as a pulse was unusually high since it seemed to want to classify everything (except sums of sines) as a pulse. These results might not be very reliable because an overly simplistic classification algorithm was used (normalized correlation with ground truth). The algorithm should be tested in conjunction with a classification algorithm more in line with those used in Fleet operations. Finally, a brief description was given of a procedure to produce an algorithm that performs better than this one.

7. ACKNOWLEDGMENTS

This work was funded by the Office of Naval Research and the Naval Research Laboratory.

REFERENCES

1. M.K. Broadhead, R.L. Field, and J.H. Leclere, "Sensitivity of the Deconvolution of Acoustic Transients to Green's Function Mismatch," *J. Acoust. Soc. Am.* **94**, 994-1002 (1993).
2. R.A. Wiggins, "Minimum Entropy Deconvolution," *Geoexplor.* **16**, 21-35 (1978).
3. M.K. Broadhead, "Broadband Source Signature Extraction from Underwater Acoustics Data with Sparse Environmental Information," *J. Acoust. Soc. Am.* **97**, 1322-1325 (1995).
4. M.K. Broadhead, L.A. Pflug, and R.L. Field, "Minimum Entropy Filtering for Improving Nonstationary Sonar Signal Classification," Proceedings of the 8th IEEE Signal Processing Workshop on Statistical Signal and Array Processing, Corfu, Greece, June 24-26, 1996, pp. 222-225.

5. M.K. Broadhead and L.A. Pflug, "Performance of Some Sparseness Criterion Blind Deconvolution Methods in the Presence of Noise," *J. Acoust. Soc. Am.* **107**, 885-895 (2000).
6. A.T. Walden, "Non-Gaussian Reflectivity, Entropy, and Deconvolution," *Geophys.* **50**, 2862-2888 (1985).
7. J.A. Cadzow, "Blind Deconvolution via Cumulant Extrema," *IEEE Signal Process. Magazine* **13**, 24-42 (1996).
8. M.K. Broadhead, L.A. Pflug, and R.L. Field, "Use of Higher Order Statistics in Source Signature Estimation," accepted for publication, *J. Acoust. Soc. Am.* (2000).
9. C.A. Cabrelli, "Minimum Entropy Deconvolution and Simplicity: A Noniterative Algorithm," *Geophys.* **50**, 394-413 (1984).
10. R.L. Field and J.H. Leclere, "Measurements of Bottom-Limited Ocean Impulse Responses and Comparisons with the Time Domain Parabolic Equation," *J. Acoust. Soc. Am.* **93**, 2599-2616 (1993).
11. E. Rietsch, "Euclid and the Art of Wavelet Estimation, Part I: Basic Algorithm for Noise-Free Data," *Geophys.* **62**(6), 1931-1946 (1997).